

A STATISTICAL PATH LOSS MODEL FOR IN-HOME UWB CHANNELS

*Saeed S. Ghassemzadeh, Rittwik Jana
Christopher W. Rice, William Turin*

AT&T Labs-Research

{saeedg, rjana, cwrice, wt}@att.com

Vahid Tarokh

Massachusetts Institute of Technology
Cambridge, MA 02139
Vahid@mit.edu

ABSTRACT

This paper describes a simple statistical model for evaluating the path loss in residential environments. It consists of detailed characterization of path loss model parameters of Ultra-Wideband Band (UWB) signals having a nominal center frequency of 5 GHz. The proposed statistical path loss model is for in-home channel and it is based on over 300,000 frequency response measurements. Probability distributions of the model parameters for different location are presented. Also, time domain results such as RMS delay spread and percent of captured power are presented.

1. INTRODUCTION

A new development in wireless communications known as Ultra-Wideband Band (UWB) radio is currently receiving a great deal of global attention. The FCC currently defines a UWB signal as any signal where its -20 dB bandwidth is at least 25% of the center frequency [1]. The techniques for generating UWB signals for radar applications have been around for several decades. Like other wireless air interface technologies, UWB may also be used for wireless LANs. For example, if approved by FCC, it could be used as an extension of IEEE 802.11 (i.e., transmissions rates in excess of a few 100 Mbps). The motivation for research in this paper stemmed from possible usage of UWB technology for distribution of broadband services inside homes. To design an air interface accommodating such a high data rate using UWB, such as the one proposed in [2], required understanding of the UWB channel inside homes.

Indoor signal propagation has been studied extensively in the past by many researchers, but these works mainly apply to bandwidths much narrower than those for UWB (see [3]-[7]). The UWB propagation measurements sited in [8]-[10] [9] have been performed mainly in industrial buildings and not for residential environment. The residential results, if it has been performed, are not in the public domain or the channels do not qualify as UWB

channels because of their transmission bandwidth or they are not at a center frequency of interest. Therefore, performing in-home measurements for understanding the behavior of the UWB signals in residential environment was inevitable. We performed an extensive amount of measurements in various home structures. The experiments shed a lot of interesting results on UWB signal propagation in different homes that is discussed in this paper. Particularly, we report some key findings of our research and propose a statistical model for evaluation of the UWB propagation path loss in residential environment.

The organization of the paper is as follows: Section 2 presents the measurement equipment and procedures; Section 3 presents the results of time domain analysis; Section 4 describes the large scale fading; and Section 5 concludes the paper.

2. EQUIPMENT AND PROCEDURES

2.1. Equipment

Fig. 1 illustrates the transceiver configurations for the channel sounder. A Vector Network Analyzer (VNA) is used for measuring the frequency response of the channel. The VNA generates a signal as the input to a variable attenuator and a 34 dB gain broadband transmitter RF amplifier chain. The output of the RF power amplifier is propagated by a vertically polarized, conical monopole, omni-directional (in the H-plane) over the 4.375 – 5.625 GHz frequency range. The signal, from the received identical conical monopole antenna, is first passed through a Low Noise Amplifier (LNA) and a gain of 34 dB. It is then returned to VNA via 150 feet long coaxial cable with 17 dB loss followed by another LNA with gain of 36 dB. High quality doubly shielded cable was used to insure no leakage from the air into the receiver by the cable. The VNA records the variation of 401 complex tones across the above-mentioned frequency range. The VNA sweeps the frequency range for 401 received tones and compares them to pre-calibrated coefficients. The sweep rate for all tones is slightly over 400 ms corresponding to maximum

measurable Doppler shift of about 2.5 Hz. The complex Data from the VNA was stored on a laptop computer via GP-IB interface.

2.2. Procedures

Using the above-mentioned hardware, experiments were performed inside 23 homes in the northern and central New Jersey area. The homes had differing structure, age, size and clutter. The transmit antenna from the VNA was always located in a fixed position, and the dual receiving antenna mast was moved throughout the houses on a pre-measured grid. Knowledge of the physical distance between the transmitter and the receiver allowed the measured data to be correlated with the distance. For all measurements, the height of the transmit/receive antennas was fixed at 1.8 m (6-feet).

Measurements were made with the transmit/receive antennas within Line-of-Sight (LOS) and within non-LOS (NLOS) of each other (see Fig. 2). Two different experiments were performed in each home. In 15 homes, we selected over 20 LOS locations and over 20 NLOS locations. We then measured the channel frequency response observed from two antennas separated by 3 feet simultaneously, over a 1.8-minute period (273 snapshots). In the each of the other 8 homes, we used only one receive antenna, 10 LOS, and 10 NLOS locations. Hence, our database contains about 1240×273 measurements of the channel frequency response. The transmit antenna location was placed for best signal coverage inside each home and optimized for minimum possible T-R separation for NLOS experiments. The transmitter’s power level was adjusted so that the VNA always operated within the linear range of its detectors and well above noise floor.

3. TIME DOMAIN ANALYSIS

3.1. Data Reduction

An estimate of the channel impulse response is made by: first removing the VNA calibration data from the measured frequency data, and then performing IDFT of that response. Finally, the impulse response is appropriately normalized such that the area under the squared-magnitude of the impulse response is equal to one.

Part of the PDP characterization is based on RMS delay spread τ_{RMS} , which is a measure of multipath spread within the channel. It is the square root of the second central moment of the PDP and is given by:

$$\tau_{RMS} = \sqrt{\sum_{i=1}^L (\tau_i - \tau_m)^2 |h(t, \tau_i)|^2} \quad (1)$$

$$\tau_m = \sum_{i=1}^L \tau_i \cdot |h(t, \tau_i)|^2$$

Here τ_m is the mean excess delay (the first moment of the PDP). τ_{RMS} is an important parameter for characterizing time dispersion or frequency selectivity.

Over 300,000 PDPs were collected and analyzed. We found that:

- Windowing improves the dynamic range of the time domain measurement by filtering the frequency response, prior to taking its IDFT, producing an impulse stimulus that has lower side-lobes but wider pulse width. However, it may increase RMS delay spread and number of multipaths within a profile as reported in [11]. Two sets of frequency response measurements were made; first with 401 samples over 1.25 GHz in 15 homes and second experiment with 801 samples over 2.5 GHz in 8 homes. Kaiser window of $\beta=5.1$, was used to lower the received pulse side lobes by better than 40-dB in the data samples of the latter experiment. Using this value of β , increased the system resolution to 0.8 ns corresponding to the same pulse width of non-windowed data of the first experiment. The mean excess delay τ_m and the RMS delay spread τ_{RMS} for both experiments were estimated. The results showed no significant increase in τ_m or τ_{RMS} .
- The values of τ_m and τ_{RMS} are normally distributed over all homes, with mean values of 4.7 ns and 8.2 ns and standard deviation values of 2.3 ns and 3.3 ns, in LOS and NLOS, respectively. See Fig. 3.
- τ_{RMS} increases as $d^{0.26}$ and $d^{0.36}$ in LOS and NLOS, respectively. See Fig. 4.
- The mean τ_{RMS} and mean path loss were obtained by averaging over 273 profiles loss for each location at each home. A comparison of their values over 23 homes indicates an increase in τ_{RMS} with increasing path loss. This anticipated increase in τ_{RMS} is largely due to the paths with longer delays having larger path loss values associated with them. See Fig. 5.
- No significant excess delay above 70 ns was observed for a 30 dB threshold.
- τ_m and τ_{RMS} were compared as a function of a threshold level in dB (i.e., -5, -10, -15, -20 and -30) below the maximum return, for the 50% and 90% population of the data. A summary of these values is given in Table 2. The results showed that the mean excess delay and RMS delay spread increases as expected. Furthermore, These observations were consistent with some frequency domain measurements reported in [11].
- The power in each multipath could be collected and combined coherently to improve received signal power. The percent power contained above a threshold level along with the number of paths, L , carrying this power, the mean excess delay, τ_m , and RMS delay spread, τ_{RMS} , was computed. Fig. 6 illustrates the percent of the energy

contained within L strongest independent return paths. Clearly, the strongest return does not carry significant power with respect to the other returns in NLOS locations. This indicates that in general the same scatterers generate most returns, and that the paths pass through the same clutters. As a result, they arrive at the receiver with powers that are comparable with each other.

4. LARGE-SCALE FADING

4.1. The Path Loss Model

The VNA removes all front-end gains and losses up to the antennas and measures the received power relative to input power. This is the total received power collected from all the paths. Clearly, if a UWB receiver is unable to collect all of this received power, it will suffer on additional path loss. This allows using the measured frequency response data, $H(f_i, t_j; d)$, for estimating the average path loss at any distance, d , by using:

$$PL(d) = \frac{1}{MN} \sum_{i=1}^N \sum_{j=1}^M |H(f_i, t_j; d)|^2 \propto d^\gamma \quad (2)$$

where N is the number of observed frequencies and M is the number of frequency response snap shots over time at d meters. It is well known that the median of this path loss can be modeled as directly proportional to d raised to some exponent γ . The path loss in dB at some distance d is then:

$$PL(d) = PL_o + 10 \cdot \gamma \log_{10} \left(\frac{d}{1\text{m}} \right) + S(d) \quad (3)$$

where PL_o , the intercept point, is the path loss (i.e., PL_o in dB) at $d=1$ m, $10\gamma \cdot \log_{10}(d/d_o)$ is the mean path loss referenced to 1 m; γ is referred to as the path loss exponent which depends on the structure of the home; and S is the lognormal shadow fading in dB.

Fig. 7 shows the scatter plot of the path loss as a function of T-R separation for all homes. Equation (3) states that, on a logarithmic scale the path loss corresponds to a straight line with a slope γ . This straight line provides the mean value of the random path loss. This amounts to fitting a least squares linear regression line through the scatter of measured path loss points in dB such that the root mean square deviation of path loss points about the regression line is minimized. Random shadowing effects of the channel occur at locations where the T-R separation is the same but have different levels of clutter in their propagation paths. This random variable usually has a normal distribution. Fig. 8 shows the distribution of shadow fading random variable S in a typical home. The normal distribution regression line fit to the dB values confirms the log-normality of shadow fading in one typical

home among the 23 homes we have measured, which has been accepted by many researchers such as in [3]-[4],[7]-[9],[11], and [12].

We can model the path loss in two different ways. First approach is to find the values of PL_o , γ , and S for the global population (i.e., the data from all homes pooled together.) in equation (3). The second approach is to find a separate pairs of (PL_o , γ , and σ) for each home and then find how those pairs are distributed over all homes (i.e., treat each parameter as a random variable). Since the standard deviation of shadow fading and the path loss exponent changes from one home to another, we chose the second approach. In the following section, we characterize the variables PL_o , γ , and σ for equation (2) for the in-home UWB path loss model.

4.2. Characterization of the Model Parameters

In order to characterize the model parameters over the all homes, the probability distributions of the parameters have to be found. The distribution of the parameters of equation (2) is as follows:

The Intercept Point, PL_o : The intercept point depends on the materials blocking the signal within 1m of T-R separation and the home structure. The measured values of PL_o for NLOS were very close to that of LOS path loss plus a few dB more loss due to the obstacle(s) blocking the LOS path. For ease of modeling, we excluded the frequency dependency of this parameter. Therefore, for LOS and NLOS, we chose the intercept value to be the mean path loss at 1m measured in 23 homes.

The σ Parameter: Over the population of our data, we note that the values of σ vary from one home to another. The values of σ have normal distribution $N[\mu_\sigma, \sigma_\sigma]$, whose mean μ_σ and standard deviation σ_σ are determined statistically from the measured data. Fig. 9 illustrates the distribution of standard deviation of shadow fading σ in all homes.

The γ Parameter: The values of γ also change from one home to another and have a normal distribution $N[\mu_\gamma, \sigma_\gamma]$. Fig. 10 depicts the distribution of the path loss exponent, γ . The statistical values for PL_o , γ and σ are presented in Table 1. These values were comparable with results found for wideband indoor channels in the literature with the exception of shadowing. By inserting these values one can use equation (3) as a path loss model for in-home UWB channel.

5. CONCLUSION

We have reported on a program of extensive measurement, data reduction and modeling of the path loss

for in-home UWB channel. The results are based on over 300,000 frequency response profiles measured in 23 homes. We have presented findings on RMS delay spread and percent of captured power, and have derived a statistical model for UWB path loss in home environment. The model gives a very simple way of generating the path loss.

6. REFERENCES

[1] FCC document 00-163, "Revision of part 15 commission rules ET Docket No. 98-153 regarding UWB transmission systems", adopted 5-10-2000.

[2] D. Gerakoulis, P. Salmi, S.S. Ghassemzadeh, "An Ultra Wide Bandwidth System For In-Home Wireless Networking", Accepted for publication in European Wireless Conference, 2002, Italy.

[3] R.J.C. Bultitude, S.A. Mahmoud, W.A. Sullivan, "A Comparison of indoor radio propagation characteristics at 910 MHz and 1.75 GHz", *IEEE J. Select. Areas Commun.*, 7:20-30, Jan 1989.

[4] T.S. Rappaport, S.Y. Seidel, K. Takamizawa, "Statistical Channel Impulse Response Models for Factory and Open Plan Building Radio Communication System Design", *IEEE Transaction on Commun.*, 39:794-806, May 1991.

[5] S.S. Ghassemzadeh, V. Erceg, D.L. Schilling, M. Taylor, H. Arshad, "Indoor Propagation and Fading Characterization of Spread Spectrum Signal at 2 GHz", *IEEE Globecom*, 92.

[6] S.S. Ghassemzadeh, D.L. Schilling, Z. Hadad, "On the Statistics of Multipath Fading Using a Direct Sequence CDMA signal at 2 GHz", *International Journal on Wireless Information Networks*, April 1994.

[7] S.J Howard, K. Pahlavan, "Measurement and Analysis of the indoor radio channel in the frequency domain", *IEEE Trans. Instrum. Measure.*, 39:751-755, Oct. 1990.

[8] M.Z. Win, R.A. Scholtz, M.A. Barnes, "Ultra-Wide Bandwidth Signal Propagation For Indoor Wireless Communications", *Proc. of IEEE Int. Conf. Commun.*, 1:56-60, June 1997.

[9] D. Cassioli, A. Molisch, M.Z. Win, "A Statistical Model for UWB Indoor Channel", *Proceedings of the IEEE VTC Spring 2001*, 2001 Rhodes.

[10] K. Siwiak, A. Petroff, "A Path Link Model For Ultra Wide Band Pulse Transmissions", *Proceedings of the IEEE VTC Spring 2001*, 2001 Rhodes.

[11] R. Addler, D. Cheung, E. Green, M. Ho, Q. Li, C. Prettie, L. Rusch, K. Tinsley, "UWB Channel

Measurements for the Home Environment", UWB Intel Forum, 2001 Oregon.

[12] V. Erceg, L. Greenstein, S. Tjandra, S. Parkoff, A. Gupta, B Kubic, A. Julius, R. Bianchi "An Empirically Based Path Loss Model for Wireless Channels in Suburban Environments", *IEEE J. Select. Areas Commun.*, 17:1205-1211, July 1999.

Table 1. Statistical values of the path loss parameters.

	LOS		NLOS	
	Mean	Std. Dev.	Mean	Std. Dev.
PL_o (dB)	47	NA	51	NA
γ	1.7	0.3	3.5	0.97
σ (dB)	1.6	0.5	2.7	0.98

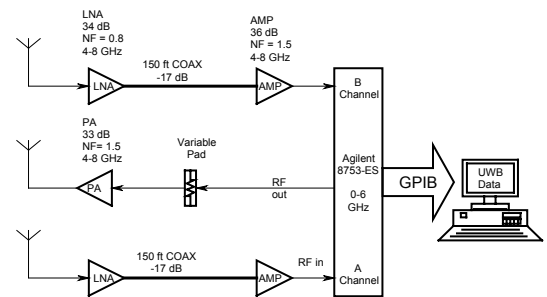


Fig. 1: Transceiver Configuration.

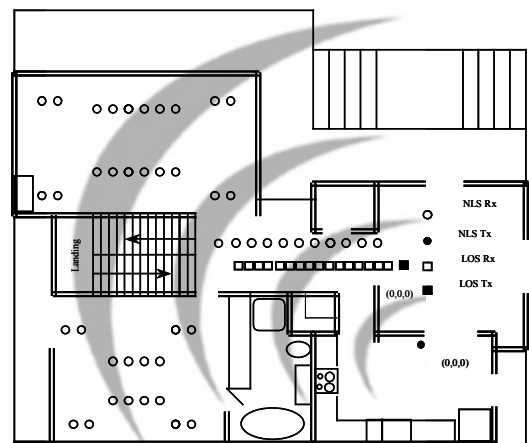


Fig. 2: Typical home layout and experiment setup.

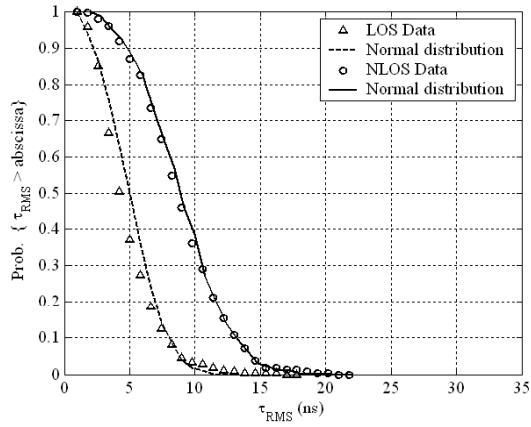


Fig. 3: CDF of RMS delay spread.

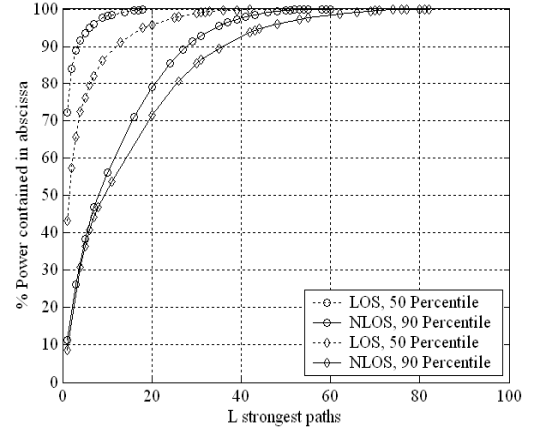


Fig. 6: Percent of power contained in strongest paths.

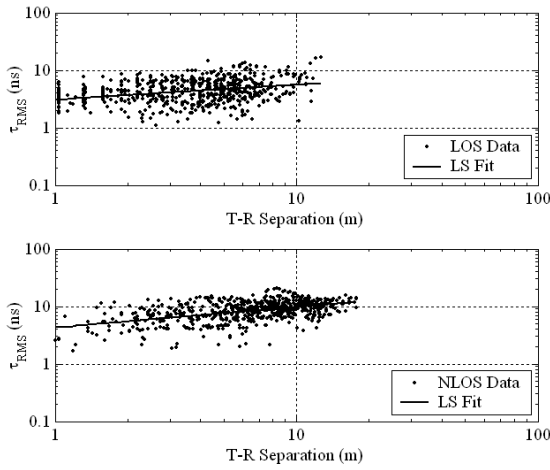


Fig. 4: RMS delay spread versus T-R separation.

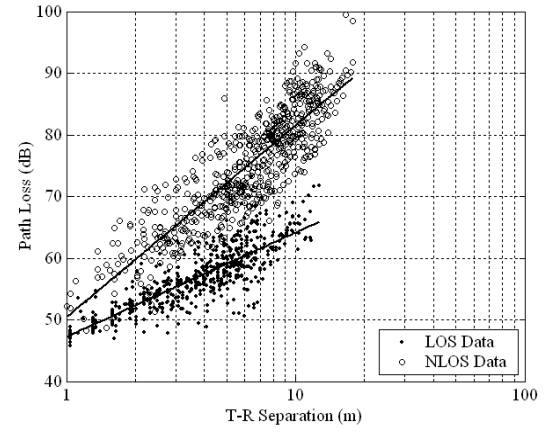


Fig. 7: Scatter plot of path loss versus T-R separation.

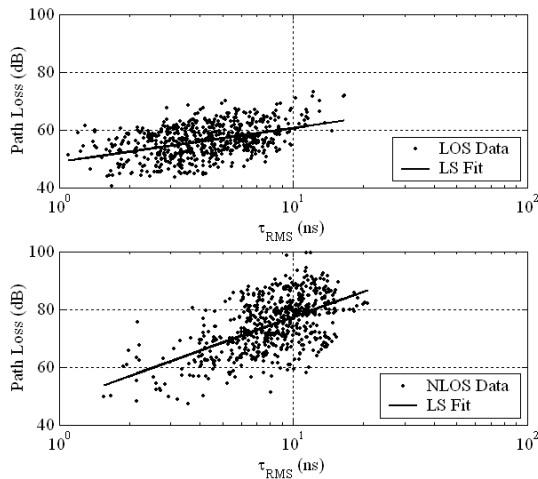


Fig. 5: Mean path loss versus RMS delay spread.

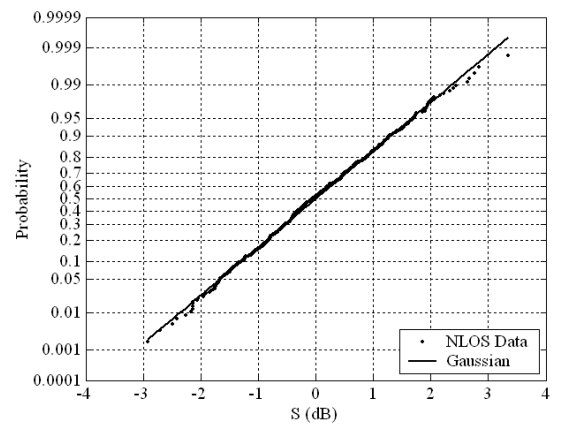


Fig. 8: CDF of shadow fading in a typical home.

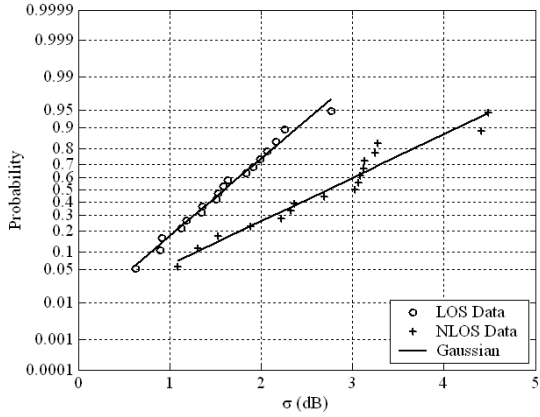


Fig. 9: CDF of standard deviation of shadow fading.

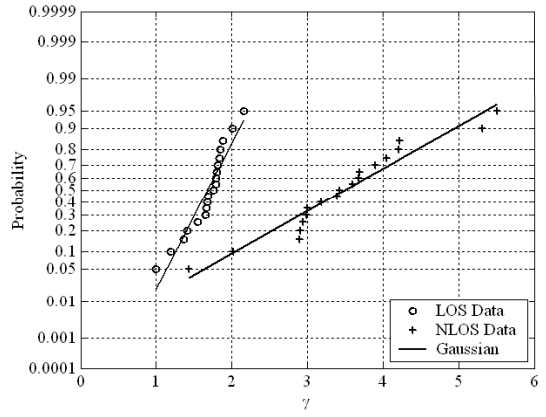


Fig. 10: CDF of path loss exponents.

Table 2. Percent of power contained in profile, Number of Paths, Mean Excess delay and RMS delay spread for 5, 10, 15, 20 and 30 dB threshold level.

Threshold	50 % NLOS				90 % NLOS			
	% Power	L	τ_m (ns)	τ_{RMS} (ns)	% Power	L	τ_m (ns)	τ_{RMS} (ns)
5-dB	46.8	7	1.95	1.52	46.9	8	2.2	1.65
10-dB	89.2	27	7.1	5.77	86.5	31	8.1	6.7
15-dB	97.3	39	8.6	7.48	96	48	10.3	9.3
20-dB	99.4	48	9.87	8.14	99.5	69	12.2	11
30-dB	99.97	60	10.83	8.43	99.96	82	12.4	11.5